



Cite this: *J. Mater. Chem. C*, 2017, 5, 3932

## Adjustable electrical characteristics in hybrid Si/PEDOT:PSS core/shell nanowire hetero-junctions†

Wenhui Lu,<sup>\*a</sup> Shuai Zhang,<sup>a</sup> Enqi Dai,<sup>a</sup> Bin Miao,<sup>b</sup> Yiran Peng,<sup>c</sup> Tao Pang,<sup>a</sup> Tiansheng Zhang,<sup>a</sup> Lei Yan,<sup>id c</sup> Shuxin Zhang,<sup>c</sup> Jiadong Li<sup>\*bd</sup> and Xingzhu Wang<sup>id \*c</sup>

Si/PEDOT:PSS core/shell nanowire hetero-junctions with adjustable electrical characteristics are reported. They exhibit an ohmic behavior ascribed to p-type Si/PEDOT:PSS, whereas n-type Si/PEDOT:PSS displays a rectifying nature. A large interfacial area within the core/shell nanowire configuration is beneficial for charge transport, decreasing the resistance by 60% for p-type Si/PEDOT:PSS, and increasing the rectification ratio by 10 times for n-type Si/PEDOT:PSS as compared to the planar structure. By incorporating a perfluorinated ionomer into PEDOT:PSS, the reverse saturation current densities of n-type Si/PEDOT:PSS core/shell nanowire hetero-junctions are reduced by 2 to 4 orders of magnitude, and the rectification performances are enhanced.

Received 22nd January 2017,  
Accepted 13th March 2017

DOI: 10.1039/c7tc00376e

rsc.li/materials-c

### Introduction

Si nanowires are attractive and promising building blocks for nano-electronic or nano-photoelectronic devices because of their unique morphology and excellent physical properties. Until now, various nano-scale devices based on Si nanowires, such as field-effect transistors,<sup>1</sup> solar cells,<sup>2</sup> photodetectors,<sup>3</sup> chemical and biological sensors,<sup>4</sup> photoelectrochemical cells,<sup>5</sup> lithium batteries<sup>6</sup> and thermoelectric devices<sup>7</sup> have been successfully demonstrated. Within various devices, the ohmic contact of Si nanowires is the key factor accounting for the device performance. The interface states between the Si nanowire and the metal contact often lead to Fermi-level pinning, resulting in a relatively large Schottky barrier, and therefore, obstruction to forming the ohmic contact. In order to address this issue, various metals are usually deposited on the Si nanowire as contact electrodes and undergo high temperature annealing to form the silicide alloy eventually, which can provide a very low Schottky barrier height between silicides/Si hetero-junctions and hence facilitates the ohmic contact.<sup>8–12</sup> However, ohmic contact requires annealing at high temperatures, which limits the choice of material and processes

for such devices. On the other hand, the Si nanowire based on a rectifying junction is essential for devices, and employs excellent rectification performance as well as simple fabrication processes.

Poly(3,4-ethylenedioxythiophene):poly(styrenesulfonate) (PEDOT:PSS), an organic conducting polymer, displays excellent optoelectronic properties such as high conductivity, and high transparency, and can be processed within various substrates at low temperature. The work function of PEDOT:PSS is about 5.1 eV, similar to the valence energy band of Si; thus, the interface between the PEDOT:PSS layer and p-type Si nanowires potentially leads to ohmic contact. In addition, the conformal coating of the PEDOT:PSS film on n-type Si nanowires could facilitate the formation of a hybrid Schottky junction,<sup>13–16</sup> which is applicable in various nano-photoelectronic devices, such as solar cells<sup>17,18</sup> and photoelectrochemical cells.<sup>19,20</sup> However, the optimization of devices requires a further improvement in the rectification performance of the hybrid core/shell nanowire hetero-junctions. For planar PEDOT:PSS/n-type Si hetero-junctions, a high work function capping layer upon the PEDOT:PSS layer can be used to induce a stronger inversion layer in the Si underneath,<sup>21–23</sup> resulting in an improved rectification performance. In principle, a similar approach would also be effective in coating the hybrid core/shell nanowires; however, a conformal coating of overlayers on the high density core/shell nanowire arrays could be a challenge.

In this work, hybrid p-type and n-type Si/PEDOT:PSS core/shell nanowire hetero-junctions were fabricated *via* a low temperature process, and their electrical characteristics were investigated. The objective of this study is not only to demonstrate the ohmic behaviour of p-type Si/PEDOT:PSS core/shell nanowire hetero-junctions, but also to enhance the rectification performance of the n-type Si/PEDOT:PSS core/shell nanowire hetero-junctions. The advantages of hybrid Si/PEDOT:PSS hetero-junctions with the

<sup>a</sup> Department of Applied Physics, College of Science, Huzhou University, Huzhou, Zhejiang 313000, P. R. China. E-mail: whlv2016@189.cn

<sup>b</sup> i-LAB, Suzhou Institute of Nano-Tech and Nano-Bionics, Chinese Academy of Sciences, Suzhou, 215125, P. R. China. E-mail: jdli2009@sinano.ac.cn

<sup>c</sup> Key Laboratory of Polymeric Materials & Application Technology of Hunan Province, College of Chemistry, Xiangtan University, Xiangtan, Hunan 411105, P. R. China. E-mail: xzwang@xtu.edu.cn

<sup>d</sup> State Key Laboratory of Applied Optics, Changchun Institute of Optics, Fine Mechanics and Physics, Chinese Academy of Sciences, 130033 Changchun, P. R. China

† Electronic supplementary information (ESI) available. See DOI: 10.1039/c7tc00376e

core/shell nanowire configuration is evaluated as compared to the planar structure. Moreover, the n-type Si/PEDOT:PSS core/shell nanowire hetero-junction exhibits an enhanced rectification performance by including a perfluorinated ionomer (PFI) into PEDOT:PSS. The corresponding physical mechanism is also discussed.

## Experimental

The hybrid p-type and n-type Si/PEDOT:PSS nanowire arrays were prepared by Ag-assisted chemical etching<sup>24</sup> followed by a PEDOT:PSS solution filling and drying approach<sup>25</sup> (for details see the ESI,† Note S1). For the p-type Si/PEDOT:PSS samples, Au electrode patterns with 400 nm thickness and  $1.1 \times 0.3 \text{ cm}^2$  area were thermally evaporated on the core/shell nanowire arrays through a shadow mask. Arrays in the spacing between the two Au contact patterns were removed by mechanical scratching. For the n-type Si/PEDOT:PSS samples, a back electric contact was applied to the backside of the samples with a 400 nm thick Al layer, and the front contact of PEDOT:PSS with a 400 nm thick Au layer. In order to provide a comparison, the planar p-type or n-type Si/PEDOT:PSS hetero-junctions have been fabricated *via* an identical experimental protocol to that mentioned above.

The morphologies of Si nanowire arrays and Si/PEDOT:PSS core/shell nanowire arrays are characterized by field emission scanning electron microscopy (FE-SEM) and transmission electron microscopy (TEM). The current–voltage characteristics of the hybrid hetero-junctions were measured using a Keithley 2400 sourcemeter. All measurements were performed at room temperature.

## Results and discussion

The Si/PEDOT:PSS core/shell nanowire arrays are illustrated in Fig. 1(a), showing that the PEDOT:PSS layer is conformal on the Si nanowires. The FE-SEM images corresponding to the prepared Si and Si/PEDOT:PSS core/shell nanowire arrays are provided in Fig. 1(b) and (c), respectively. It is observed that the Si nanowires stand on the Si substrate. The formation mechanism adopted by the Si nanowires was assumed to be driven by the Si electro-chemical reaction within HF and H<sub>2</sub>O<sub>2</sub> solutions, as described in a previous report.<sup>26</sup> Once the film of PEDOT:PSS has undergone coating, the tops of the nanowires are interconnected. The morphology of the Si/PEDOT:PSS core/shell nanowires have been further confirmed by the TEM image as depicted in Fig. 1(d), indicating clearly the core/shell nature of the nanowire structure. The diameter of the core/shell nanowires has been found to be within the range of 30–180 nm.

Fig. 2 shows the typical current–voltage curves of the hybrid p-type Si/PEDOT:PSS core/shell nanowire hetero-junctions in comparison with the planar p-type Si/PEDOT:PSS hetero-junction. The current–voltage curves corresponding to both the planar and nano-structured p-type Si/PEDOT:PSS hetero-junctions exhibit the ohmic behavior at low voltage ranges between the two Au contact patterns with different spacings. The result demonstrates the formation of ohmic contact between the PEDOT:PSS layer and

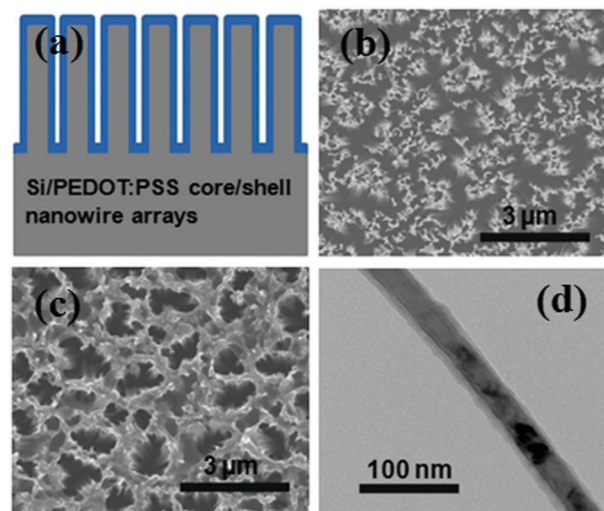


Fig. 1 (a) Schematic illustration of the hybrid Si/PEDOT:PSS core/shell nanowire arrays; (b) FE-SEM image of the Si nanowire arrays; (c) FE-SEM image of the Si/PEDOT:PSS core/shell nanowire arrays; and (d) TEM image of a single Si/PEDOT:PSS core/shell nanowire.

p-type Si nanowires. The underlying mechanism has been ascribed to the similar energy level of the work function of PEDOT:PSS and the Si valence energy band. However, a deviation of both planar and nano-structured p-type Si/PEDOT:PSS hetero-junctions from the ohmic behavior was monitored at high voltage ranges. The physical mechanism for this is still not understood.

To further evaluate the ohmic contact characteristics, the total resistances between the two Au contact patterns were plotted as a function of contact spacing (see the inset in Fig. 2). The total resistance is as described by the following equation:

$$R_T = 2R_c + \frac{R_{\square-\text{Si}} \times d}{L} \quad (1)$$

in which  $R_T$  is the total resistance between the two Au contact patterns,  $R_c$  is the resistance of p-type Si/PEDOT:PSS core/shell nanowire arrays between the Au electrode and Si substrate,  $R_{\square-\text{Si}}$  is the sheet resistance of the Si substrate,  $L$  is the length of the Au contact pattern, and  $d$  is the spacing between the Au contact patterns. Thus,  $R_c$  was determined using eqn (1) to linearly fit the experimental plot. The results show that the resistance of the p-type Si/PEDOT:PSS core/shell nanowire arrays between the Au electrode and the Si substrate with an effective area of  $0.33 \text{ cm}^2$  has decreased by 60% as compared to the planar p-type Si/PEDOT:PSS/Au contact. The corresponding specific contact resistance,  $\rho_c = L_c^2 R_{\square-\text{Si}}/4$ , has decreased by 77%. This behaviour originates from a large interfacial contact area for the charge transport in the core/shell nanowire configuration that directly connects the Si nanowires with the Si substrates. Therefore, the p-type Si/PEDOT:PSS hetero-junctions with core/shell nanowire configuration have the potential to induce a lower contact resistance.

Fig. 3(a) illustrates the typical current density–voltage curves of the hybrid n-type Si/PEDOT:PSS hetero-junctions with planar as well as core/shell nanowire configurations. They all exhibited a rectifying behavior. The current density of the hybrid core/shell

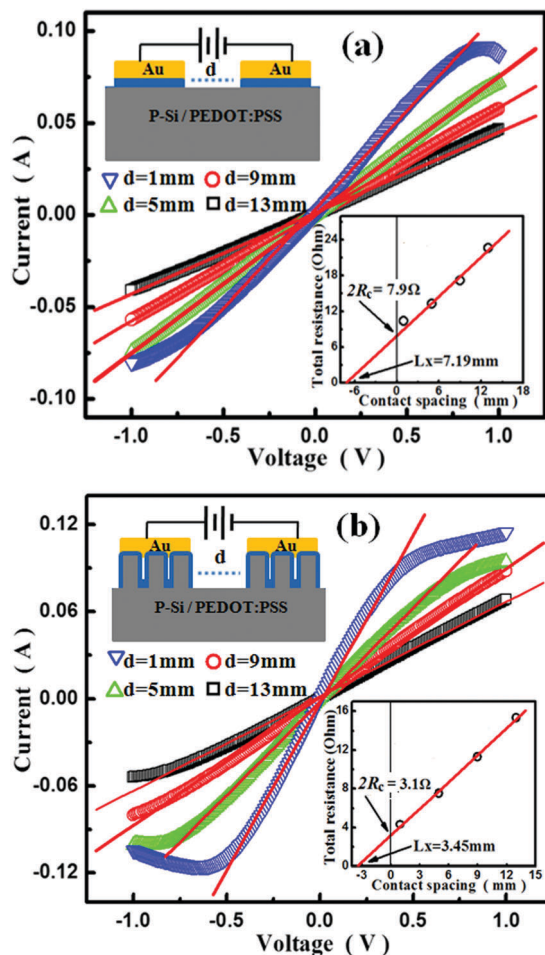


Fig. 2 (a) The current–voltage curves between the two Au contact pattern with different spacing for the hybrid planar p-type Si/PEDOT:PSS hetero-junctions, and (b) the current–voltage curves between the two Au contact patterns with different spacings for the hybrid core/shell nanowire p-type Si/PEDOT:PSS hetero-junctions; inset:  $R_T$ – $d$  behavior extracted from the current–voltage measurements for the hybrid planar p-type Si/PEDOT:PSS hetero-junctions in (a), and  $R_T$ – $d$  behavior extracted from the current–voltage measurements for the hybrid core/shell nanowire p-type Si/PEDOT:PSS hetero-junctions in (b).

nanowire hetero-junctions at a positive bias was enhanced as compared to the hybrid planar ones. However, the current density at the negative bias has displayed similar orders of magnitude for both types. Thus, the rectifying ratio at 1 V of the hybrid core/shell nanowire hetero-junction has increased by more than 10 times as compared to the hybrid planar samples. The results suggest that the junction configurations play a key role in determining the current density–voltage curves. When the Si nanowire is just at full depletion, the built-in potential in the Si nanowires in hybrid n-type Si/PEDOT:PSS hetero-junctions is approximately described by the following equation (for details see the ESI,<sup>†</sup> Note S2):

$$V_D = \int_0^{r_0} E dr = \frac{qN_D}{4\epsilon_0\epsilon_r} r_0^2 \quad (2)$$

where  $V_D$  is the built-in potential in Si nanowires,  $q$  is the elementary charge,  $\epsilon_0\epsilon_r$  are the dielectric constants of Si,

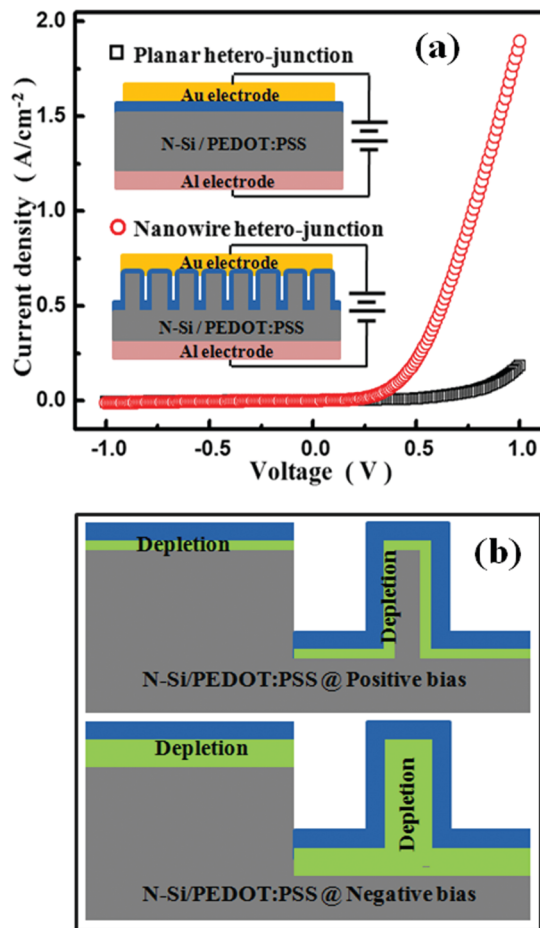


Fig. 3 (a) Typical current density–voltage curves of the hybrid n-type Si/PEDOT:PSS hetero-junctions with planar (black squares) and core/shell nanowire configuration (red circles); (b) schematic depletion region profiles at a positive bias and a negative bias for both the planar and nano-structured n-type Si/PEDOT:PSS hetero-junctions.

$N_D = 2.4 \times 10^{15} \text{ cm}^{-3}$  is the doping concentration of Si, and  $r_0$  is the radius of the Si nanowires. At the equilibrium state, the built-in potential in the Si nanowires is more than 0.45 eV.<sup>13–16</sup> According to eqn (2),  $r_0$  is more than 693 nm. In the hybrid n-type Si/PEDOT:PSS core/shell nanowire hetero-junctions, the radius of the Si nanowires is less than 693 nm, resulting in full depletion of Si nanowires at the equilibrium state. When an increased positive bias is applied to the hybrid hetero-junction, the built-in potential in the Si nanowires is reduced. Then the Si nanowires will change from being fully depleted to partially depleted. In contrast, when increased negative bias is applied to the hybrid hetero-junction, the built-in potential in the Si nanowires is enhanced. Then the Si nanowires will be further depleted. Therefore, schematic depletion region profiles at a positive bias and a negative bias for both the planar and nano-structured n-type Si/PEDOT:PSS hetero-junctions are shown in Fig. 3(b). At a positive bias, the core/shell nanowire hetero-junctions have displayed larger work interfacial contact area than the planar ones due to distinct morphologies of the junctions, offering charge transfer channels. Based on this observation, an enhanced forward

current density within the core/shell nanowire hetero-junctions can be expected. At the negative bias, the Si nanowires may be completely depleted because of their smaller diameter. Thus, the hybrid n-type Si/PEDOT:PSS planar and core/shell nanowire hetero-junctions have a similar work interfacial area for charge transfer at the negative bias, resulting in almost the same reverse current density. Therefore, the n-type Si/PEDOT:PSS hetero-junctions with core/shell nanowire configuration are beneficial to get a large rectification ratio.

The hybrid n-type Si/PEDOT:PSS hetero-junctions are considered as Schottky diodes because of the metallic properties of PEDOT:PSS. A Schottky diode employs the thermionic emission of the majority carriers over the Schottky barrier as the transport mechanism; and its current density–voltage features are described by the ideal diode eqn (3) and (4):

$$J = J_0 \left\{ \exp \left[ \frac{q}{nkT} (V - JAR_s) \right] - 1 \right\} + \frac{V - JAR_s}{AR_{sh}} \quad (3)$$

$$J_0 = A^* T^2 \exp \left( -\frac{q\phi_B}{kT} \right) \quad (4)$$

where  $k$  is the Boltzmann constant,  $T$  is the absolute temperature,  $J$  is the current density,  $V$  is the applied voltage,  $J_0$  is the reverse saturation current density,  $n$  is the diode ideality factor,  $A$  is the effective area,  $R_s$  is the series resistance,  $R_{sh}$  is the shunt resistance,  $A^*$  is called the Richardson constant, and  $\phi_B$  is the barrier height of the Schottky diode.  $J$  and  $J_0$  are mainly dependent on  $\phi_B$ , which is defined as the potential difference between the band edge of the semiconductor and the Fermi energy of the metal for an ideal Schottky diode, consisting of an n-type semiconductor and a metal. Hence, the Fermi work function of the PEDOT:PSS plays an important role in the rectification performance of the hybrid Schottky diode, especially in the current density at a negative bias.

Bearing the purpose in mind of verifying the hypothesis described above as well as enhancing the rectification performance of the hybrid Schottky diode, different amounts of a perfluorinated ionomer (PFI) have been added into PEDOT:PSS, facilitating the adjustment of the Fermi work function of the conducting polymer composition.<sup>27,28</sup> The PFI solution was purchased from Aldrich Co. (No. 527084). PFI solutions at volumetric ratios of 0:3, 1:3, 2:3, and 3:3 were added to the PEDOT:PSS solution to eventually fabricate the hybrid n-type Si/PFI-modified PEDOT:PSS core/shell nanowire hetero-junctions. The resulting hetero-junctions have revealed a clear difference within the current density–voltage curves as shown in Fig. 4. All hetero-junctions have exhibited a rectifying behavior; however, a significant drop in the reverse current density at negative bias was recorded as the content of PFI was increased. As a consequence of this observation, the rectification ratios of the hybrid n-type Si/PFI modified PEDOT:PSS core/shell nanowire hetero-junctions at 1 V have been enhanced by more than 1–2 orders of magnitude as compared to the ones of un-doped PEDOT:PSS (see Table 1). The explanation behind such enhanced rectification ratios is based on the dropping of the reverse saturation current density. On the other hand, the reverse saturation current densities can be obtained by the best

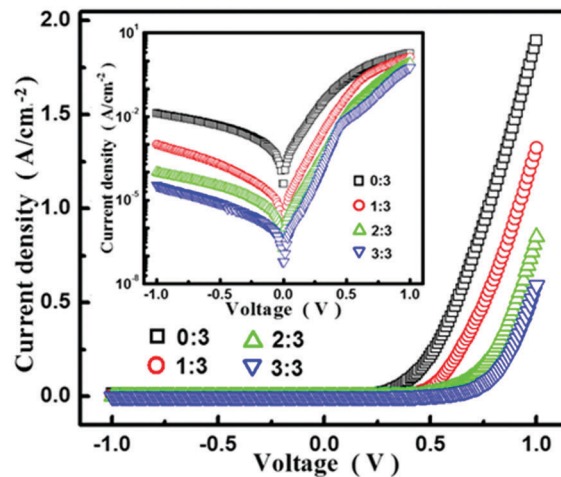


Fig. 4 The current density–voltage curves of the hybrid n-type Si/PFI modified PEDOT:PSS core/shell nanowire hetero-junctions for four different PFI/PEDOT:PSS compositions at solution volume ratios of 0:3 (black squares), 1:3 (red circles), 2:3 (green triangles) and 3:3 (blue inverted triangles); inset: the same data plotted in logarithmic scale.

fitting of the diode dominated region with  $\ln(J) = \ln(J_0) + (q/nkT)V$ . The fitting results are as summarized in Table 1. It indicates that the reverse saturation current densities decrease as the content of PFI increases. The reverse saturation current density is reduced by 2–4 orders of magnitude due to the addition of PFI into PEDOT:PSS. As previously reported,<sup>27</sup> the Fermi work function of the conducting polymer has expanded with the increase of the PFI content, which can be used to enhance the Schottky barrier height of the hybrid n-type Si/PFI modified PEDOT:PSS core/shell nanowire hetero-junctions. According to eqn (4), the reduced reverse saturation current densities also suggest that the Schottky barrier height of the hybrid hetero-junctions was improved by PFI addition, corroborating the above discussion. At a reverse bias, electrons will have to overcome the Schottky barrier from the PEDOT:PSS to Si, and form a reverse current. The electrical transport mechanism<sup>29,30</sup> includes thermal emissions, thermionic field emissions, as well as non-ideal effects. A higher Schottky barrier height can cause a lower reverse current. Therefore, the physical mechanism facilitating reduced reverse current density and enhanced rectification ratios can be attributed to the Schottky barrier height which was improved by PFI addition.

The p-type Si/PEDOT:PSS core/shell nanowires exhibit better ohmic behaviour and can be obtained *via* a simple low temperature process, and thus are promising materials and structures for Si-based nano-electronic devices. In addition, an effective way has been demonstrated to promote the rectification performance of the hybrid n-type Si/PEDOT:PSS core/shell nanowire

Table 1 Rectification ratio and  $J_0$  of the hybrid n-type Si/PFI modified PEDOT:PSS core/shell nanowire hetero-junctions for different composition ratios of PFI and PEDOT:PSS

PFI: PEDOT (v/v)	0:3	1:3	2:3	3:3
Rectification ratio	$1.4 \times 10^2$	$1.3 \times 10^3$	$8.0 \times 10^3$	$1.8 \times 10^4$
$J_0$ (A cm <sup>-2</sup> )	$2.6 \times 10^{-4}$	$8.1 \times 10^{-6}$	$1.3 \times 10^{-6}$	$9.1 \times 10^{-8}$

hetero-junctions, which is beneficial for the performance of organic-inorganic hybrid photoelectronic devices, such as solar cells.

## Conclusions

In summary, hybrid p-type and n-type Si/PEDOT:PSS core/shell nanowire hetero-junctions were fabricated and their electrical characteristics were investigated. The results showed that such materials exhibited an ohmic nature for the p-type/PEDOT:PSS, whereas the n-type Si/PEDOT:PSS displayed a rectifying behavior. The core/shell nanowire configuration over the planar structure is beneficial for charge transport, resulting in a lower resistance for the p-type and a higher rectification ratio for the n-type Si/PEDOT:PSS hetero-junctions. Furthermore, the n-type Si/PEDOT:PSS core/shell nanowire hetero-junctions exhibited a reduced reverse saturation current density and an enhanced rectification performance by including PFI into PEDOT:PSS. The hybrid core/shell nanowire hetero-junctions achieved *via* a simple low temperature fabrication process with tailored electrical characteristics represent a promising platform for application in organic-inorganic hybrid electronic devices or photoelectronic devices.

## Acknowledgements

This work was supported by the National Natural Science Foundation of China (No. 61204068, 51473139), the Natural Science Foundation of Zhejiang Province (No. LY15F040002), and the Natural Science Foundation of Huzhou University (No. 2014XJKY48). W. Lu thanks the Fund of Key Laboratory of Optoelectronic Materials Chemistry and Physics, CAS (No. 2008DP173016). J. Li thanks The Youth Innovation Promotion Association CAS and the Fund of State key Laboratory of Applied Optics, Changchun institute of Optics, Fine Mechanics and Physics, CAS. X. Wang thanks the Open Project of Hunan Provincial University Innovation Platform (14k092) and Hunan 2011 Collaborative Innovation Center of Chemical Engineering & Technology with Environmental Benignity and Effective Resource Utilization for the financial support and the Xiangtan University Undergraduate Innovative Experiment Program.

## Notes and references

- 1 Y. Cui, Z. Zhong, D. Wang, W. U. Wang and C. M. Lieber, *Nano Lett.*, 2003, **3**, 149–152.
- 2 B. Z. Tian, X. L. Zheng, T. J. Kempa, Y. Fang, N. F. Yu, G. H. Yu, J. L. Huang and C. M. Lieber, *Nature*, 2007, **449**, 885–888.
- 3 C. Yang, C. J. Barrelet, F. Capasso and C. M. Lieber, *Nano Lett.*, 2006, **6**, 2929–2934.
- 4 Y. Cui, Q. Q. Wei, H. K. Park and C. M. Lieber, *Science*, 2001, **293**, 1289–1292.
- 5 A. P. Goodey, S. M. Eichfeld, K. K. Lew, J. M. Redwing and T. E. Mallouk, *J. Am. Chem. Soc.*, 2007, **129**, 12344–12345.
- 6 C. K. Chan, H. L. Peng, G. Liu, K. Mcilwrath, X. F. Zhang, R. A. Huggins and Y. Cui, *Nat. Nanotechnol.*, 2008, **3**, 31–35.
- 7 A. I. Hochbaum, R. Chen, R. D. Delgado, W. Liang, E. C. Garnett, M. Najarian, A. Majumdar and P. Yang, *Nature*, 2008, **451**, 163–167.
- 8 N. S. Dellas, C. J. Schuh and S. E. Mohney, *Nano Lett.*, 2009, **9**, 410–415; N. S. Dellas, C. J. Schuh and S. E. Mohney, *J. Mater. Sci.*, 2012, **47**, 6189–6205.
- 9 B. Z. Liu, Y. F. Wang, S. M. Dilts, T. S. Mayer and S. E. Mohney, *Nano Lett.*, 2007, **7**, 818–824.
- 10 Y. C. Lin, K. C. Lu, W. W. Wu, J. Bai, L. J. Chen, K. N. Tu and Y. Huang, *Nano Lett.*, 2008, **8**, 913–918.
- 11 S. M. Woodruff, N. S. Dellas, B. Z. Liu, S. M. Eichfeld, T. S. Mayer, J. M. Redwing and S. E. Mohney, *J. Vac. Sci. Technol., B: Microelectron. Nanometer Struct. – Process., Meas., Phenom.*, 2008, **26**, 1592–1596.
- 12 N. S. Dellas, B. Z. Liu, S. M. Eichfeld, C. M. Eichfeld, T. S. Mayer and S. E. Mohney, *J. Appl. Phys.*, 2009, **105**, 094309.
- 13 Y. J. Lin, B. C. Huang, Y. C. Lien, C. T. Lee, C. L. Tsai and H. C. Chang, *J. Phys. D: Appl. Phys.*, 2009, **42**, 165104.
- 14 M. J. Price, J. M. Foley, R. A. May and S. Maldonado, *Appl. Phys. Lett.*, 2010, **97**, 083503.
- 15 F. T. Zhang, T. Song and B. Q. Sun, *Nanotechnology*, 2012, **23**, 194006.
- 16 W. H. Lu, Q. Chen, B. Wang and L. W. Chen, *Appl. Phys. Lett.*, 2012, **100**, 023112.
- 17 S. C. Shiu, J. J. Chao, S. C. Hung, C. L. Yeh and C. F. Lin, *Chem. Mater.*, 2010, **22**, 3108–3113.
- 18 Y. F. Zhang, W. Cui, Y. W. Zhu, F. S. Zu, L. S. Liao, S. T. Lee and B. Q. Sun, *Energy Environ. Sci.*, 2015, **8**, 297–302.
- 19 T. Yang, H. Wang, X. M. Ou, C. S. Lee and X. H. Zhang, *Adv. Mater.*, 2012, **24**, 6199–6203.
- 20 X. J. Li, W. H. Lu, W. L. Dong, Q. Chen, D. Wu and L. W. Chen, *Nanoscale*, 2013, **5**, 5257–5261.
- 21 R. Y. Liu, S. T. Lee and B. Q. Sun, *Adv. Mater.*, 2014, **26**, 6007–6012.
- 22 X. H. Mu, X. G. Yu, D. K. Xu, X. L. Shen, Z. H. Xia, H. He, H. Y. Zhu, J. S. Xie, B. Q. Sun and D. R. Yang, *Nano Energy*, 2015, **16**, 54–61.
- 23 J. He, P. Q. Gao, Z. H. Ling, L. Ding, Z. H. Yang, J. C. Ye and Y. Cui, *ACS Nano*, 2016, **10**, 11525–11531.
- 24 M. L. Zhang, K. Q. Peng, X. Fan, J. S. Jie, R. Q. Zhang, S. T. Lee and N. B. Wong, *J. Phys. Chem. C*, 2008, **112**, 4444–4450.
- 25 W. H. Lu, C. W. Wang, W. Yue and L. W. Chen, *Nanoscale*, 2011, **3**, 3631–3634.
- 26 K. Q. Peng, A. J. Lu, R. Q. Zhang and S. T. Lee, *Adv. Funct. Mater.*, 2008, **18**, 3026–3035.
- 27 T. W. Lee, O. Kwon, M. G. Kim, S. H. Park, J. Chung, S. Y. Kim, Y. Chung, J. Y. Park, E. Han, D. H. Huh, J. J. Park and L. Pu, *Appl. Phys. Lett.*, 2005, **87**, 231106.
- 28 D. J. D. Moet, P. D. Bruyn and P. W. M. Blom, *Appl. Phys. Lett.*, 2010, **96**, 153504.
- 29 S. M. Sze, *Physics of semiconductor devices*, Wiley, New York, 1981.
- 30 A. Varonides, *Phys. Status Solidi C*, 2016, **13**, 1040–1044.